European Journal of Pharmaceutics and Biopharmaceutics 130 (2018) 115–122

Contents lists available at ScienceDirect

European Journal of Pharmaceutics and Biopharmaceutics

journal homepage: www.elsevier.com/locate/ejpb

Research paper

Semi-interpenetrated, dendritic, dual-responsive nanogels with cytochrome *c* corona induce controlled apoptosis in HeLa cells

Enrico Miceli[a,b], Stefanie Wedepohl[a], Ernesto Rafael Osorio Blanco[a], Guido Noé Rimondino[c,d], Marisa Martinelli[d,e], Miriam Strumia[d,e], Maria Molina[a], Mrityunjoy Kar[a], Marcelo Calderón[a,b,*]

[a] *Freie Universität Berlin, Institute of Chemistry and Biochemistry, Takustr. 3, 14195 Berlin, Germany*
[b] *Helmholtz Virtual Institute "Multifunctional Biomaterials for Medicine", Kantstr. 55, 14513 Teltow, Germany*
[c] *Instituto de Investigaciones en Físico Química de (INFIQC), CONICET, Departamento de Físico-Química, Facultad de Ciencias Químicas, Universidad Nacional de Córdoba, Córdoba, Argentina*
[d] *Universidad Nacional de Córdoba, Facultad de Ciencias Químicas, Departamento de Química Orgánica, LaMaP Laboratorio de Materiales Poliméricos, Haya de la Torre y Medina Allende, X5000HUA Córdoba, Argentina*
[e] *CONICET. Instituto de Investigación y Desarrollo en Ingenieria de Procesos y Química Aplicada (IPQA-Conicet), Argentina*

A B S T R A C T

The use of thermoresponsive nanogels (NGs) allows the controlled release of therapeutic molecules upon a thermal switch. Usually, this strategy involves the use of temperature increase to activate cargo expulsion from shrinking NGs. In this study, poly(N-isopropylacrylamide) (pNIPAM)-based NGs were involved in the release of a therapeutic protein corona by temperature decrease. NGs based on dendritic polyglycerol (dPG) and thermoresponsive pNIPAM were semi-interpenetrated with poly(4-acryloylamine-4-(carboxyethyl)heptanodioic acid) (pABC). The resulting semi-interpenetrated NGs retain the thermoresponsive properties of pNIPAM, together with pH-responsive, dendritic pABC as a secondary network, in one single nanoparticle. Semi-interpenetrated polymer network (SIPN) NGs are stable in physiological conditions, exhibit a reversible phase transition at 35 °C, together with tunable electrophoretic mobilities around the body temperature. The binding of cytochrome *c* (cyt *c*) was successful on SIPN NGs in their collapsed state at 37 °C. Upon cooling of the samples to room temperature, the swelling of the NG effectively boosted the release of cyt *c*, as compared with the same kept at constant 37 °C. These responsive SIPN NGs were able to deliver cyt *c* to cancer cells and specifically induce apoptosis at 30 °C, while the cells remained largely unaffected at 37 °C. In this way, we show therapeutic efficacy of thermoresponsive NGs as protein carriers and their efficacy triggered by temperature decrease. We envision the use of such thermal trigger as relevant for the treatment of superficial tumors, in which induction of apoptosis can be controlled by the application of local cooling agents.

1. Introduction

Nanogels (NGs) are three-dimensional crosslinked nanoparticles that are able to absorb a large amount of water. They constitute a class of new nanocarriers for the loading and improved release *in situ* of hydrophilic cargoes (both small molecules or macromolecules) in controlled conditions. Their ease of functionalization with dyes or inorganic imaging agents allows them to be used as powerful diagnostic agents, in an effort to combine therapeutic efficacy and diagnostics in one single theranostic macromolecule [1,2]. Their nanosized dimensions allow for an increased residence time in the bloodstream by avoiding excretion from the kidneys [3], as well as for enhanced skin [4] and follicular penetration [5] or improved mucosal adhesion [6]. Stimuli-responsive NGs are capable of changing their physicochemical properties upon exposure to external conditions such as temperature, pH, reducing conditions, light, and magnetic field, among others. These "smart" materials offer new promising perspectives for the development of next generation agents for the controlled delivery of drugs [7,8]. Thermoresponsive polymers exhibit a reversible phase transition, caused by the hydrophobic aggregation upon heating of their aqueous solutions to temperatures above their lower critical solution temperature (LCST). Poly(N-isopropylacrylamide) (pNIPAM) undergoes this phase transition at around 33 °C [9]. Thermoresponsive NGs based on N-isopropylacrylamide (NIPAM) are one of the main candidates for biomedical research due to their reversible phase transition at a temperature of 33 °C, close to the body temperature [10]. pNIPAM NGs

* Corresponding author at: Freie Universität Berlin, Institute of Chemistry and Biochemistry, Takustr. 3, 14195 Berlin, Germany.
E-mail address: marcelo.calderon@fu-berlin.de (M. Calderón).

https://doi.org/10.1016/j.ejpb.2018.06.023
Received 7 November 2017; Received in revised form 14 June 2018; Accepted 18 June 2018
Available online 19 June 2018
0939-6411/

crosslinked with dendritic polyglycerol (dPG) [11], were published by our group, showing a versatility for their use in biomedical applications. The copolymerization of pNIPAM with poly(N-isopropylmethacrylamide) (pNIPMAM) or hydrophilic comonomers, such as acrylamide or acrylic acid, helps tuning the LCST values to a more desired transition temperature, closer to 37 °C [12,13]. The use of dPG as a macromolecular crosslinker helps improving the biocompatibility of pNIPAM, as well as avoiding the pNIPAM-driven NG aggregation above the LCST, thus ensuring the colloidal stability of dPG-pNIPAM NGs under physiological conditions [11]. The high swelling abilities of NGs can be exploited to achieve high loadings of bioactives [14]. This property, combined with the abrupt shrinkage of the thermoresponsive network upon temperature change, gives NGs unique properties for the controlled release of small drugs, as well as biomacromolecules, in a controlled fashion.

Dendrons are molecules with regular branching points and symmetrical tree-like structures. At their extremity, the repeated end groups may induce multivalency, leading to an exponential increase in binding affinities [15,16]. In some cases though, multivalency is counteracted by steric crowding which may hinder the multivalent effects, leading to a binding saturation point, in an anti-cooperative fashion [17–19]. The tuning of the generation (number of repeated branchings) allows the regulation of the hydrophilic/hydrophobic balance of the dendron [20]. In this way, the binding affinity towards guest molecules can be tuned, whether these are small molecules, proteins, dendrons, or polymers [21]. Newkome-type dendrons/dendrimers are a class of molecules that are biocompatible, non-toxic and are used to create polymers with multifunctional acidic units, useful for promoting host-guest interactions with therapeutically relevant moieties [22–27]. Among this class of dendrons, 4-acryloylamine-4-(carboxyethyl)heptanodioic acid (ABC) and its copolymer NGs with pNIPAM have been developed by our group and have been proven to provide sustained release of cisplatin at lysosomal conditions [28]. Following a similar approach, we used ABC in this study to generate semi-interpenetrated NGs with dendritic multifunctional units that can be used as anchoring points for the binding of therapeutic proteins. Semi-interpenetrated polymer networks (SIPNs) are composed by more than one polymeric network that are physically entangled, although not covalently bound to each other. Due to the entanglement, the different networks cannot be separated by simple mechanical stress, but rather only by chemical reactions. This approach is useful for the fabrication of polymer composites that retain the physicochemical properties of the individual independent networks and maintain stable polymer compositions. SIPN NGs can be synthesized by a two-step process, in which the secondary network is being polymerized inside the preformed NG. By controlling the synthetic parameters of the polymerization, the resulting SIPN concentrations can be modified in order to get chain lengths that can be optimized to achieve maximum SIPN surface exposure upon shrinkage of the thermoresponsive NG scaffolds. Our group has developed dPG-pNIPAM SIPN NGs with polymerized 2-acrylamido-2-methylpropane sulfonic acid (AMPS) or dimethylaminoethyl methacrylate (DMAEM) as vectors for the efficient delivery of doxorubicin to the resistant KB-V1 cell line [29]. Their incorporation into honeycomb films for controlled bovine serum albumin (BSA) delivery was investigated and described by our group in a follow-up study [30]. Their copolymeric NG analogues were reported in another case study for the sustained delivery of doxorubicin and methotrexate [31]. In another report, we employed dPG-PNIPAM SIPN NGs with poly (aniline) as secondary network, a near infrared - active polymer to add photothermal reactivity to the NGs [32]. Several other examples of SIPN NGs can be found in literature, showing a broad range of applications for this synthetic approach, for the development of next generation nanoparticles for biomedical applications [33–37].

The use of protein drugs has advantages over conventional chemotherapy agents, due to their inherent lower toxicities combined with high specificities. The presence of a protein corona has a profound impact on the biological efficacy of nanoparticles, and by designing tailor-made protein corona one could boost the therapeutic efficacy of the nanoparticles [38,39], in a synergistic effort to combine efficient nanosized vectors to therapeutic proteins [40]. Cytochrome *c* (cyt *c*) is a small, 12 kDa heme protein with an isoelectric point (pI) of 10 and is therefore positively charged at a physiological pH of 7.4. In cells, cyt *c* is loosely associated to the inner membrane of the mitochondria and is involved as an intermediate in the electron transport chain. If released into the cytosol, cyt *c* triggers apoptosis by binding to apoptosis activating factor-1 (Apaf-1). This in turn is responsible for the activation of caspase-9 to initiate the intrinsic apoptotic cascade [41,42]. While cyt *c* itself is membrane-impermeable, recent studies involved the use of nanoparticles (NPs) for sustained cytosolic release of cyt *c*. Different nanoparticle-based systems have been evaluated for the activation of apoptosis following cyt *c* release: mesoporous SiO_2 NPs [43] or a combination of end-capped cyt *c* and encapsulated doxorubicin [44], crosslinked cyt *c* – based NPs [45] or redox-sensitive hyaluronic acid NGs [46,47]. To our knowledge however, none of these studies investigate the temperature-dependent cyt *c* activation for controlled induction of apoptosis.

In this work, we describe the synthesis of dendritic SIPN NGs, based on thermoresponsive dPG-pNIPAM NGs, with pABC as a SIPN (Fig. 1).

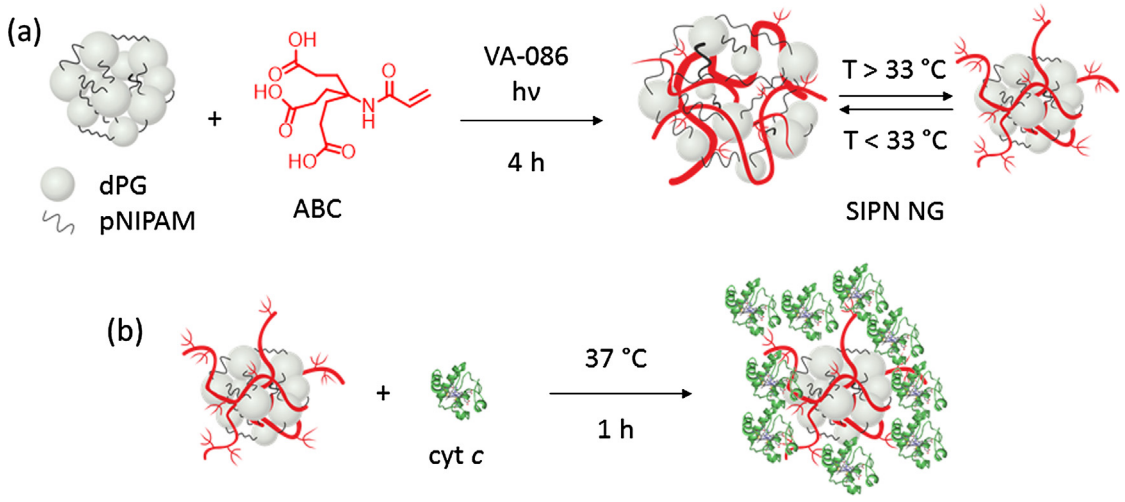

Fig. 1. (a) Schematic representation of the polymerization of 4-acryloylamine-4-(carboxyethyl)heptanodioic acid inside the preformed dendritic polyglycerol - poly (N-isopropylacrylamide) nanogels. (b) Generation of cyt *c* – loaded nanogels.

This arrangement forms NGs which maintain the original thermoresponsiveness of pNIPAM, together with dPG to provide colloidal stability at a temperature higher than the pNIPAM LCST (33 °C), combined with pH-sensitive dendritic pABC or monofunctional control poly (acrylic acid) (pAA) as SIPN. We characterized the NGs via UV–VIS, nuclear magnetic resonance spectroscopy (NMR), dynamic light scattering (DLS) and acid-base titration. These NGs were loaded with cyt *c* at 37 °C, to boost the preferential formation of a corona around the collapsed NG, which was mediated by binding pABC or pAA on the NG surface. The subsequent swelling of the NGs at 25 °C was investigated in relation with its ability to disrupt the binding, thereby triggering the release of cyt *c*. The temperature-controlled delivery of cyt *c* was evaluated *in vitro* in HeLa cells, where the ability of the cyt *c*-laden NGs to induce apoptosis by controlled intracellular delivery of cyt *c* was probed. In this way, we combined dendritic NG design with the use of a thermal trigger in order to achieve full control on the reactivity of a therapeutic protein. Thus, we introduce a model system for the development of NG-based therapeutics for the treatment of superficial tumors or skin diseases, where local cooling may be efficiently applied.

2. Materials and methods

All materials were purchased from Sigma, except 2,2-azobis(2-methyl-N-(2-hydroxyethyl)-propionamide) (VA-086), which was purchased from Wako Ltd.

The syntheses of dPG-PNIPAM NGs and ABC have been previously published [11,28]. Briefly, for a partial acrylation of dPG, a solution of acryloyl chloride (0.22 mL, 2.7 mmol) in dry DMF (4 mL) was added to a solution of dPG (2 g, 10 kDa, 27.03 mmol −OH groups) and triethylamine (0.24 mL, 1.72 mmol) in DMF (60 mL) at 0 °C. The reaction was then allowed to run at 25 °C for 4 h. The resulting 10% dPG-Acrylate (dPG-Ac) was purified by dialysis against deionized water for 2 days (molecular weight cut-off, MWCO = 2 kDa). For the synthesis of dPG-pNIPAM NGs, NIPAM was added 2:1 w/w to dPG-Ac, together with 0.36 mg mL^{-1} sodium dodecyl sulfate (SDS), and 0.56 mg mL^{-1} APS. The mixture was transferred to a hot bath at 68 °C and the polymerization process was initiated after 5 min with the addition of a catalytic amount of tetramethylethylenediamine (TEMED) (0.16 mol L^{-1}). The mixture was stirred at 250 rpm at 68 °C under argon for 4 h. The product was dialyzed for 2 days in water using dialysis membrane (MWCO = 50 kDa) to obtain thermoresponsive NGs as a white, cotton-like powder in quantitative yields, after lyophilization.

The synthesis of SIPN NGs proceeded as follows: 50 mg of lyophilized dPG-PNIPAM NG were soaked in a 5 mL solution of ABC or AA in a concentration range of 0.3–2.6 mg mL^{-1} at 0 °C for 16 h. Lyophilized nanogels were allowed to swell inside the monomer solution to achieve the maximum monomer encapsulation efficiencies. The solution was then purified by ultrafiltration (MWCO = 1 MDa), then 2 mg VA-086 were added and the solution was purged for 30 min under Ar flow. The polymerization was then initiated by visible light irradiation for 1 min and kept running for 4 h in an ice bath. The solution was dialyzed (MWCO = 50 kDa) against water and ultimately freeze-dried, to obtain SIPN NGs as a cotton-like powder. The NGs showed stable compositions by ^{1}H NMR, showing no detectable polymer leaching out of a dialysis membrane (MWCO = 50 kDa) after 3× repeated heating/cooling cycles.

The cyt *c* binding was done by mixing 200 μL of a 20 mg mL^{-1} solution of SIPN NG and 200 μL of a 20 mg mL^{-1} cyt *c* solution both in phosphate buffered saline (PBS), for 4 h at 37 °C. The solution was then purified by ultrafiltration (MWCO = 1 MDa), by short centrifugation cycles at 5000*g* of maximum 10 s, in order to not cool down the sample, to prevent NG swelling. Repeated centrifugation and warming cycles (~30×) are needed in order to wash with 2 mL PBS volume through the cartridge. The cyt *c* amount was quantified by UV–VIS spectroscopy, by measuring absorbance at λ = 530 nm.

Hydrodynamic diameters were measured by dynamic light scattering (DLS) in a Malvern Zetasizer instrument with a He–Ne laser (λ = 633 nm) and scattering angle of 173°. All the samples were prepared at 1 mg mL^{-1} in 10 mM PBS at pH 7.4 and a 150 mM ionic strength. For ζ-potential measurements, electrophoretic mobility of the NGs was analyzed following application of a 20 V cm^{-1} electric field.

Nuclear magnetic resonance spectra (NMR) were recorded on a Bruker AVANCE III 700, 700 MHz at 25 °C or 45 °C in deuterated water. Data was analyzed using the MestreNova software package.

Transition temperatures were measured on a Cary 100 Bio UV–VIS spectrophotometer equipped with a six-position sample holder and a temperature controller. Buffer NG solutions (1 mg mL^{-1}) were heated at 0.2 °C min^{-1} while monitoring both the transmittance at 500 nm (1 cm path length) and the solution temperature (from 15 to 65 °C), as determined by the internal temperature probe. The cloud point temperature (T_{cp}) of each NG was determined using the minimum of the first derivative of the graph % transmittance vs. temperature.

Release studies were conducted inside an ultrafiltration cartridge (MWCO = 1 MDa). Fast repeated centrifugation cycles (10 s at 5000*g*) were used in order to avoid sample cooling. The collection of the filtrate at different times and quantifying cyt *c* by means of absorbance measurement at λ = 530 nm, led to the quantification of the released cyt *c*. Repeated experiments at 37 °C and 25 °C were performed by the identical procedure.

For the apoptosis assay, 1 × 10^5 HeLa cells mL^{-1} were seeded into 96 well plates and incubated overnight. The next day, the supernatant was discarded and replaced by 100 μL/well fresh medium with dilutions of compounds. The cyt *c* concentration served as the basis for dilution calculations and equal volumes of the respective unloaded NGs were applied. Samples and cells were kept at temperatures above 37 °C using a heating block and a heating plate. 10-fold serial dilutions were prepared in a 96-well plate placed on the heat plate at 40 °C. Dilutions for duplicate wells were prepared independently. Two identical plates were prepared. Incubations were done in two regular cell culture incubators set to 37 °C or 30 °C and 5% CO_2. One plate was incubated at 37 °C for 2 h (presumed uptake phase), then at 30 °C over night (release phase), then 4 h @ 37 °C (apoptosis induction phase). The other identical plate was incubated in parallel but at 37 °C only. Caspase 3/7 activity was measured using the Caspase-Glo® 3/7 Assay System (Promega) according to the instructions of the manufacturer.

3. Results

3.1. Synthesis and characterization of SIPN nanogels

The dPG-pNIPAM NGs and ABC were synthesized according to procedures published previously by our group [11,28]. In a common procedure for NG semi-interpenetration, the lyophilized dPG-pNIPAM NGs were soaked in a concentrated aqueous solution of ABC or acrylic acid (AA). ABC or AA were present in a concentration range of 0.3–2.6 mg mL^{-1} in the NGs solution (10 mg mL^{-1}). After purification by ultracentrifugation, the SIPN formation occurred *via* radical polymerization of the acrylic monomer inside the NGs. The light activation of 0.3 mg mL^{-1} 2,2′-azobis(2-methyl-N-(2-hydroxyethyl)propionamide) (VA-086) was used to initiate the radical polymerization of the SIPN. After 4 h of polymerization, the conversion of pABC or pAA in the resulting SIPN NGs was found to be in the range of 12–26%, as determined by acid-base titration with 10 mM NaOH. The low conversion values may indicate a lack of affinity between ABC or AA and dPG-pNIPAM NG scaffolds. The low conversion may also be exacerbated by the extensive sample washing of porous NGs, which was conducted in order to prevent superficial monomer residing on the NG surface and promote an SIPN formation. Table 1 shows the values obtained from characterization of a panel of SIPN NGs. Different ratios were screened to obtain SIPN with increasing concentrations inside the NGs.

The NGs exhibited unimodal distributions and maintained the typical thermoresponsive behavior of pNIPAM, showing a decrease in

Table 1
Summary of the size data for the characterization of semi-interpenetrated nanogels.

SIPN concentration[a]	Size[b], nm			
	25 °C	30 °C	37 °C	45 °C
0.2 mol% pABC	137 ± 59	134 ± 55	101 ± 26	104 ± 32
0.5 mol% pABC	130 ± 58	135 ± 51	95 ± 31	97 ± 26
0.9 mol% pABC	128 ± 56	131 ± 54	99 ± 27	92 ± 25
1.4 mol% pABC	138 ± 58	133 ± 45	103 ± 27	107 ± 33
2.7 mol% pABC	127 ± 58	128 ± 52	93 ± 22	86 ± 18
1.3 mol% pAA	132 ± 57	124 ± 47	93 ± 33	98 ± 29
1.9 mol% pAA	133 ± 61	130 ± 47	102 ± 25	107 ± 31
5.1 mol% pAA	130 ± 53	133 ± 47	126 ± 48	123 ± 54

[a] Ratio normalized to poly(N-isopropylacrylamide) content, quantified *via* acid-base titration.
[b] Measured in PBS (10 mM, pH 7.4).

volume of about 67% at 37 °C. An increase in SIPN concentration led to proportionally lower decreases in size at higher temperatures, which might be another indication for a non-thermoresponsive secondary network being increasingly exposed to the NG surface upon collapse of the pNIPAM network. In the extreme case of 5.1 mol% pAA SIPN nanogel, a size decrease upon nanogel shrinkage is negligible by DLS, supposedly due to long pAA chains that counteract the size decrease of the NG shell. UV–VIS spectroscopy revealed cloud point temperature (T_{cp}) values of 35 °C for all samples, in agreement with the values obtained by dPG-pNIPAM NGs prior to semi-interpenetration (see SI). As expected from the synthetic approach, the semi-interpenetration was not affecting the thermoresponsive behavior of the NGs. After semi-interpenetration with both pABC (pKa = 5) and pAA (pKa = 4.2), NGs exhibit temperature-dependent variations in electrophoretic mobility at a neutral pH of 7.4. By increasing the temperature above the NG's T_{cp} (35 °C), NGs turned from neutral to negatively charged. This finding was interpreted as an indication for pABC or pAA being exposed at the NGs surface after NG shrinkage. Reversible electrophoretic mobility transitions with increasing temperature were observed, for samples with at least 1.4 mol% pABC or 1.9 mol% pAA, as shown in Fig. 2. The decrease in electrophoretic mobilities was found to be around the LCST of pNIPAM, and proportional to the SIPN concentrations. In this way, the SIPN provided new temperature-dependent charge density fluctuations to the NGs, which were then exploited as on-demand switchable protein binding moieties.

By comparing ^{1}H NMR spectra of pABC SIPN NGs at 25 °C and 45 °C, at which NGs are either completely swollen or fully shrunken, the spectra revealed significant changes in the peak intensities of the different polymers. In Fig. 3 it can be visualized how the peaks representing pNIPAM (δ = 0.8–2.1; δ = 3.8 ppm) are strongly decreasing at 45 °C as compared to those detected at 25 °C. The peak intensities for dPG (δ = 3.4–3.7; δ = 3.9 ppm) and pABC at δ = 2.3 ppm remained in turn mostly constant after temperature increase. This observation corroborates the previous finding that pABC chains and dPG are surface-active after the collapse of pNIPAM.

3.2. Cyt c binding and in vitro release kinetics

The ability to expose charges on the surface of the NGs triggered by temperature change allowed the use of SIPN NGs as agents for reversible electrostatic binding of proteins. At 37 °C and pH 7.4 the NGs achieve maximum exposure of negatively charged pABC (or pAA), an ideal setting for the binding of basic proteins. A cyt *c* corona was thus easily formed, likely by electrostatic pairing of the positively charged protein with negatively charged pABC (or pAA) mostly on the NG surface. A 20 nm size increase was encountered by DLS for NGs after the binding, indicating the presence of a cyt *c* corona. Although the collapsed NGs were ideally not contributing to encapsulation, loading capacities were found to be high, with values found in a range of 50–70 w/w% for SIPN pABC NGs and 70–80 w/w% for SIPN pAA NGs, starting from an initial 1:1 w/w cyt c/NG ratio. After the cyt *c* binding, release kinetics were determined both at a constant temperature of 37 °C and by cooling down to 25 °C, to investigate whether the swelling of NGs would cause cyt *c* release. The kinetics data is shown in Fig. 4.

For pABC SIPN NGs, a distinct boost in the release was observed by cooling down the samples to 25 °C, as compared to the release values obtained at 37 °C, in samples with at least 0.9 mol% pABC. Two distinct kinetic domains can be identified, according to the adopted system temperature. In this case, the swelling of the NGs efficiently boosted the release of cyt *c*, thereby acting as a trigger. For samples having less than 0.9 mol% pABC, the SIPN concentration might have been too low to observe any difference in release kinetics, just as they did not show strong electrophoretic mobility changes above and below 32 °C (Fig. 2, right). An intermediate concentration of pABC (1.4 mol%) reached an optimal modulation for the binding of cyt *c*, showing optimal polymer length (and chemistry) for the binding to be counteracted with the mechanical swelling of the NG. A further increase of pABC length (/concentration) in SIPN NGs may increase the availability of anchoring points, increasing the electrostatic binding strength, causing deceleration of the release of cyt *c*. The same kinetics for pAA SIPN NGs

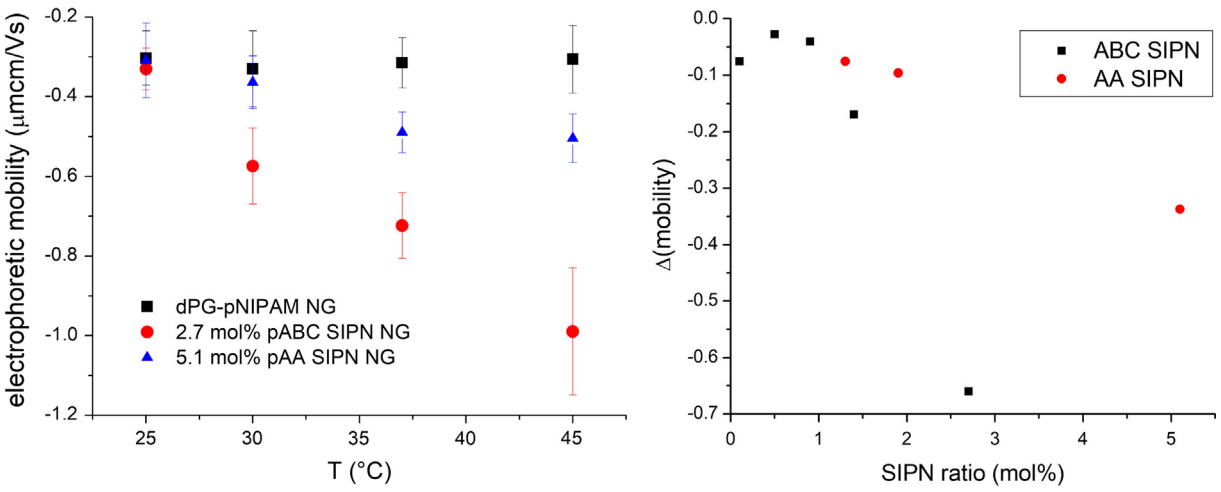

Fig. 2. Evolution of electrophoretic mobility values with temperature, measured at pH 7.4 in a 10 mM sodium phosphate buffer for dendritic polyglycerol – poly(N-isopropylacrylamide) nanogels, semi-interpenetrated poly(4-acryloylamine-4-(carboxyethyl)heptanodioic acid) and poly(acrylic acid) nanogels (left). Data is represented according to (mean ± SD) over n = 3 repeats. Differential electrophoretic mobility in the range 25–45 °C, according to SIPN concentration (right).

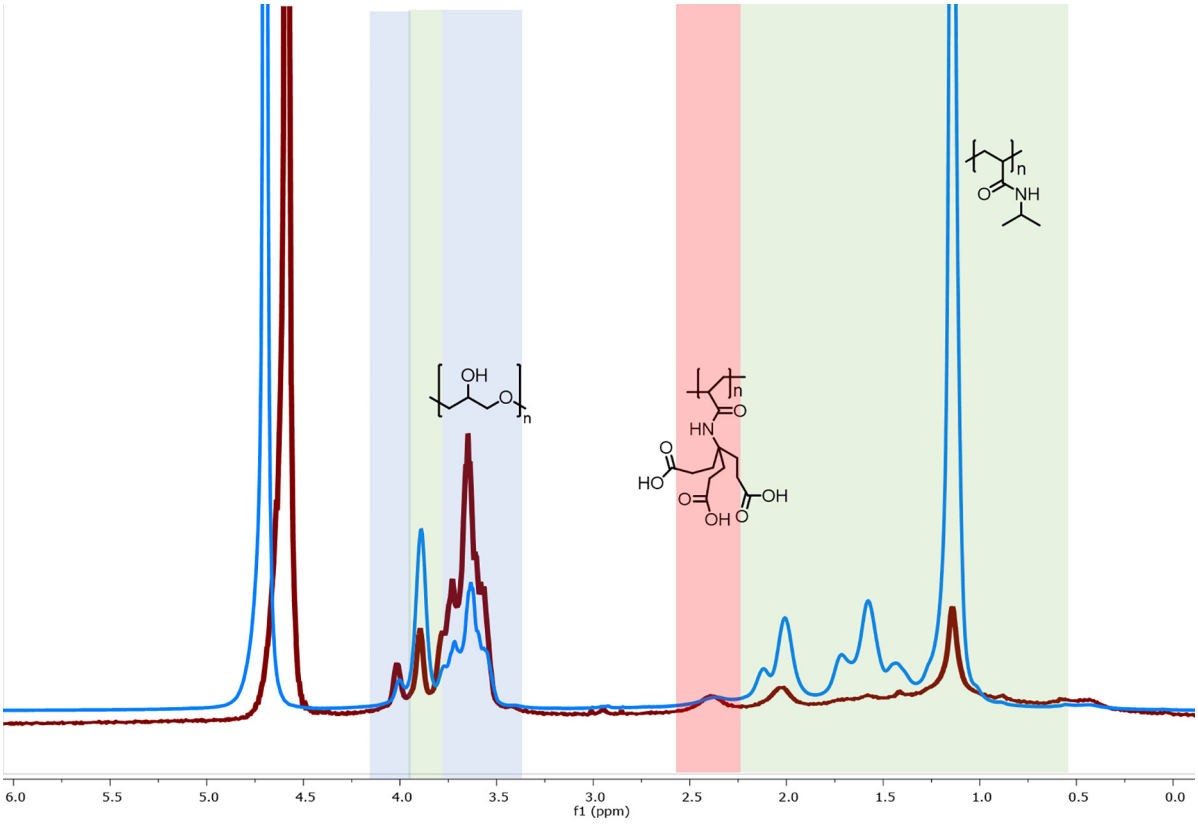

Fig. 3. ^{1}H NMR spectra in D_2O of 2.7 mol% poly(4-acryloylamine-4-(carboxyethyl)heptanodioic acid) semi-interpenetrated nanogels at 25 °C (blue line) vs 45 °C (red line). (For interpretation of the references to colour in this figure legend, the reader is referred to the web version of this article.)

however were almost independent from the experimental temperature, with a slight increase at 37 °C. Although a sustained release in a 24 h interval was still present in this case, the kinetics curves resemble those observed for cyt *c* alone or non-SIPN NGs, although with increasing half - lives (see SI). Thus, the driving force for cyt *c* release by AA SIPN NGs may be attributed to simple diffusion, with no contribution from NG swelling. For pAA-cyt *c* samples, a slower release and 25% higher loadings might indicate a stronger binding than in pABC-cyt *c* samples, with comparable SIPN polymer concentrations/−COOH groups. Control non-SIPN NGs had a lower cyt *c* loading (16 wt%) and a very fast

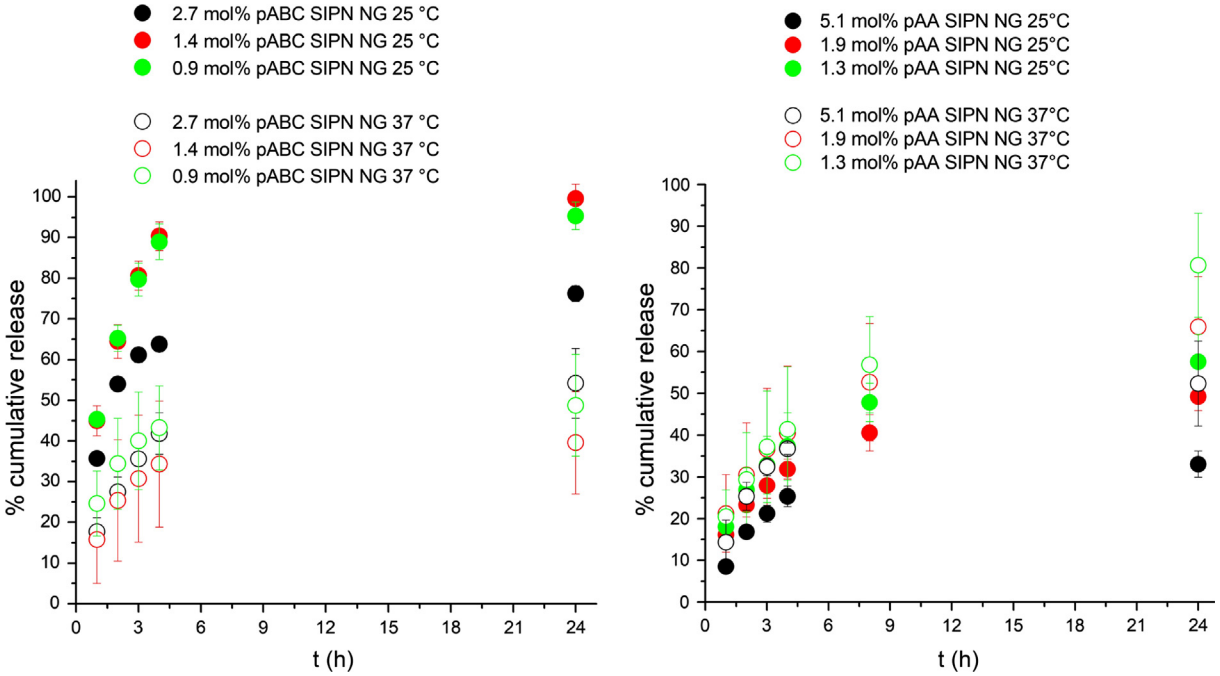

Fig. 4. Cytochrome *c* release kinetics for semi-interpenetrated poly(4-acryloylamine-4-(carboxyethyl)heptanodioic acid) nanogels (left), semi-interpenetrated poly (acrylic acid) nanogels (right). Data is represented according to (mean ± SD) over n = 3 repeats.

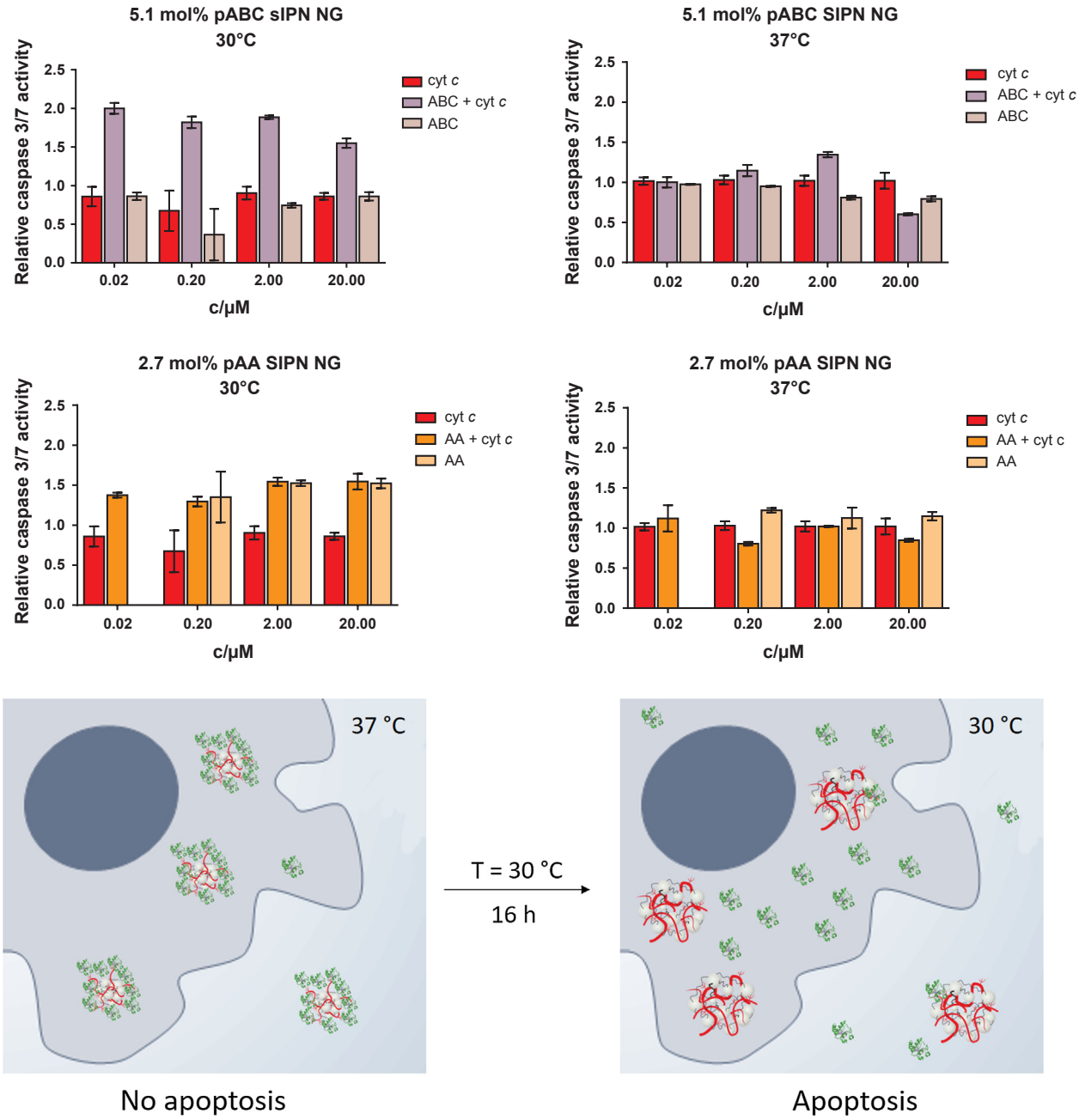

Fig. 5. Induction of apoptosis in HeLa cells after incubation with semi-interpenetrated 2.7 mol% pABC (top) and 5.1 mol% pAA nanogels (middle) at 30 and 37 °C. Relative activity was derived from caspase 3/7 activity of treated cells versus untreated control cells (medium only). Bottom panel: Cartoon representation of the proposed mode of action of cyt *c* loaded SIPN NGs. The release of cytochrome *c* from 2.7 mol% pABC nanogels was efficiently boosted by swelling of the nanogels at 30 °C, thereby activating apoptosis in HeLa cells. Data is represented according to (mean ± SD) over n = 2 repeats.

release behavior, with more than 70% cyt *c* released within 4 h, independently from the experimental temperature (see SI), indicating a lack of specific binding to cyt *c*. Furthermore, the structural integrity of cyt *c* was confirmed by circular dichroism measurements after release (see SI). Overall, the kinetics shown here by dendritic SIPN NGs, is unique and found to be reproducible among dendritic pABC samples. No other SIPN, nor other kinds of nanogels previously reported by our group or others were able to boost release by cooling, while most thermoresponsive systems do in fact the opposite.

3.3. Induction of apoptosis in HeLa cells

To confirm the controlled binding and triggered release of cyt *c* in a biological context, we investigated the ability of the loaded SIPN NGs to induce apoptosis in HeLa cells. The NGs, both loaded with cyt *c* and unloaded as a control, were first incubated at 37 °C for 2 h with HeLa cells to allow cellular uptake of the NG at the physiologically optimal temperature. Then the temperature was lowered to 30 °C, allowing a prolonged release of cyt *c* for 16 h, while a parallel sample set was kept at 37 °C, where release of cyt *c* should be strongly sustained. In the last step, all samples were incubated at 37 °C for 4 h, in order to allow sufficient time at physiologically optimal temperature for the induction of apoptosis, which was measured by quantifying caspase 3/7 activation (Fig. 5).

We could clearly observe that apoptosis was promoted only in presence of cyt *c*-loaded 2.7 mol% pABC NG, and the effect was greatly amplified at 30 °C, where full NG swelling occurred. This effect of the NG swelling had an impact on the cyt *c* release *in vitro*, which activated

apoptosis in HeLa cells. 2.7 mol% pABC SIPN NG with cyt *c* concentrations as low as 20 nM were promoting apoptosis at 30 °C, while no dose dependency was observed with increasing cyt *c* concentration. At 37 °C, a minimum cyt *c* concentration of 200 nM was necessary to observe any effect on apoptosis, which was slightly enhanced by increasing towards 2 μM cyt *c*. While a slight increase in apoptosis was generated by 5.1 mol% pAA SIPN NG, independently from the cyt *c* loading, no effect was detected in combination with cyt *c*. In this case, no efficient cytosolic delivery of cyt *c* might have occurred, possibly due to a too strong pAA-cyt *c* binding. Again, the careful choice of SIPN polymer showed an impact on the therapeutic efficacy of SIPN NGs as cyt *c* carriers for controlled apoptosis.

4. Conclusions

In this work, we synthesized SIPN NGs by a simple one-pot strategy, to achieve NGs with repetitive dendritic charged units, which were increasingly exposed to the NG surface above 35 °C. By exploiting negative charges at 37 °C, we were able to form a reversible binding of cyt *c* by electrostatic pairing with pABC. The stability of the cyt *c* – NG complex was investigated in relation with the NG swelling *in vitro*, where a boost in the release of cyt *c* was observed for SIPN pABC NGs when cooled down to room temperature. By maintaining a higher temperature of 37 °C, the cyt *c* binding was in fact more stable and the cyt *c* release was decreased. The use of a dendritic polymer (pABC) helped tuning the binding affinity to cyt *c* in order to get full on-demand control of loading/release of cyt *c* upon NG swelling, which was exploited as thermal trigger. We could demonstrate their potential for controlled delivery applications, as the loaded and released cyt *c* could successfully promote apoptosis in HeLa cells. The activation of the intrinsic apoptotic pathway following cyt *c* cytosolic delivery was observed only in presence of cyt *c*-loaded 2.7 mol% pABC SIPN NG, the effect being strongly enhanced by full NG swelling, induced by applying moderate cooling to 30 °C. We therefore achieved full controlled reactivity of dendritic SIPN NGs as carriers for the apoptotic reagent cyt *c*, its activation being regulated by a simple thermal trigger, by careful choice of dendritic SIPN polymer in modest concentrations. Moreover, such general approach may show potential for the reversible binding of other proteins of interest.

Overall, we believe that the use of localized cooling agents in combination with thermoresponsive NGs and a preassembled protein corona may show promising uses for the treatment of superficial tumors as well as skin diseases. The use of therapeutic proteins, combined with dendritic thermoresponsive NGs as macromolecular agents, may be beneficial in order to reduce side effects of conventional therapeutics as well as to improve the therapy specificity.

Acknowledgements

We gratefully acknowledge financial support from the Bundesministerium für Bildung und Forschung (BMBF) through the NanoMatFutur award (ThermoNanogele, 13N12561), DFG-CONICET, CONICET, Alexander von Humboldt foundation, the Focus Area NanoScale of the Freie Universität Berlin (http://www.nanoscale.fu-berlin.de), and the Sonderforschungsbereich 1112 (http://www.sfb1112.de), Project A04.

Declaration of interest

None.

Appendix A. Supplementary material

Supplementary data associated with this article can be found, in the online version, at https://doi.org/10.1016/j.ejpb.2018.06.023.

References

[1] D. Li, C.F. van Nostrum, E. Mastrobattista, T. Vermonden, W.E. Hennink, Nanogels for intracellular delivery of biotherapeutics, J. Control. Release 259 (2016) 16–28.
[2] M. Kar, M. Molina, M. Calderon, How are we applying nanogel composites in biomedicine? Nanomedicine 12 (2017) 1627–1630.
[3] M. Calderón, A. Sosnik, Polymeric soft nanocarriers as smart drug delivery systems: state-of-the-art and future perspectives, Biotechnol. Adv. 33 (2015) 1277–1278.
[4] M. Asadian-Birjand, J. Bergueiro, F. Rancan, J.C. Cuggino, R.C. Mutihac, K. Achazi, J. Dernedde, U. Blume-Peytayi, A. Vogt, M. Calderón, Engineering thermoresponsive polyether-based nanogels for temperature dependent skin penetration, Polym. Chem. 6 (2015) 5827–5831.
[5] F.F. Sahle, M. Giulbudagian, J. Bergueiro, J. Lademann, M. Calderón, Dendritic polyglycerol and N-isopropylacrylamide based thermoresponsive nanogels as smart carriers for controlled delivery of drugs through the hair follicle, Nanoscale 9 (2017) 172–182.
[6] A. Sosnik, J. das Neves, B. Sarmento, Mucoadhesive polymers in the design of nano-drug delivery systems for administration by non-parenteral routes: a review, Progr. Polym. Sci. 39 (2014) 2030–2075.
[7] M. Molina, M. Asadian-Birjand, J. Balach, J. Bergueiro, E. Miceli, M. Calderón, Stimuli-responsive nanogel composites and their application in nanomedicine, Chem. Soc. Rev. 44 (2015) 6161–6186.
[8] R. Cheng, F. Meng, C. Deng, Z. Zhong, Bioresponsive polymeric nanotherapeutics for targeted cancer chemotherapy, Nano Today 10 (2015) 656–670.
[9] S. Fujishige, K. Kubota, I. Ando, Phase transition of aqueous solutions of poly(N-isopropylacrylamide) and poly(N-isopropylmethacrylamide), J. Phys. Chem. 93 (1989) 3311–3313.
[10] J. Bergueiro, M. Calderon, Thermoresponsive nanodevices in biomedical applications, Macromol. Biosci. 15 (2015) 183–199.
[11] J.C. Cuggino, C.I. Alvarez, M.C. Strumia, P. Welker, K. Licha, D. Steinhilber, R.-C. Mutihac, M. Calderón, Thermosensitive nanogels based on dendritic polyglycerol and N-isopropylacrylamide for biomedical applications, Soft Matter 7 (2011) 11259–11266.
[12] J. Shen, T. Ye, A. Chang, W. Wu, S. Zhou, A colloidal supra-structure of responsive microgels as a potential cell scaffold, Soft Matter 8 (2012) 12034–12042.
[13] Y. Wang, H. Xu, J. Wang, L. Ge, J. Zhu, Development of a thermally responsive nanogel based on chitosan-poly(N-isopropylacrylamide-co-acrylamide) for paclitaxel delivery, J. Pharm. Sci. 103 (2014) 2012–2021.
[14] Y. Chen, X. Zheng, H. Qian, Z. Mao, D. Ding, X. Jiang, Hollow core-porous shell structure poly(acrylic acid) nanogels with a superhigh capacity of drug loading, ACS Appl. Mater Interf. 2 (2010) 3532–3538.
[15] C. Fasting, C.A. Schalley, M. Weber, O. Seitz, S. Hecht, B. Koksch, J. Dernedde, C. Graf, E.W. Knapp, R. Haag, Multivalency as a chemical organization and action principle, Angew. Chem. Int. Ed. Engl. 51 (2012) 10472–10498.
[16] M. Martinelli, M. Strumia, Multifunctional nanomaterials: design synthesis and application properties, Molecules 22 (2017) 243.
[17] J.W. Jones, W.S. Bryant, A.W. Bosman, R.A.J. Janssen, E.W. Meijer, H.W. Gibson, Crowned dendrimers: pH-responsive pseudorotaxane formation, J. Org. Chem. 68 (2003) 2385–2389.
[18] I. Porcar, H. Cottet, P. Gareil, C. Tribet, Association between protein particles and long amphiphilic polymers: effect of the polymer hydrophobicity on binding isotherms, Macromolecules 32 (1999) 3922–3929.
[19] S. Bhatia, D. Lauster, M. Bardua, K. Ludwig, S. Angioletti-Uberti, N. Popp, U. Hoffmann, F. Paulus, M. Budt, M. Stadtmuller, T. Wolff, A. Hamann, C. Bottcher, A. Herrmann, R. Haag, Linear polysialoside outperforms dendritic analogs for inhibition of influenza virus infection in vitro and in vivo, Biomaterials 138 (2017) 22–34.
[20] B. Devarakonda, R.A. Hill, M.M. de Villiers, The effect of PAMAM dendrimer generation size and surface functional group on the aqueous solubility of nifedipine, Int. J. Pharm. 284 (2004) 133–140.
[21] J.I. Paez, M. Martinelli, V. Brunetti, M.C. Strumia, Dendronization: a useful synthetic strategy to prepare multifunctional materials, Polymers 4 (2012) 355–395.
[22] L. Fernandez, M. Calderón, M. Martinelli, M. Strumia, H. Cerecetto, M. González, J.J. Silber, M. Santo, Evaluation of a new dendrimeric structure as prospective drugs carrier for intravenous administration of antichagasic active compounds, J. Phys. Org. Chem. 21 (2008) 1079–1085.
[23] I.P. Julieta, B. Veronica, A.C. Eduardo, C.S. Miriam, Dendritic chemistry applied to the construction of tailored functional nanomaterials: synthesis and characterization of gold nanoparticle-cored dendrimers (NCDs), Curr. Org. Chem. 17 (2013) 943–955.
[24] N. Dib, L. Fernández, L. Otero, M. Santo, M. Calderón, M. Martinelli, M. Strumia, First generation newkome-type dendrimer as solubility enhancer of antitumor benzimidazole carbamate, J. Incl. Phenom. Macrocycl. Chem. 82 (2015) 351–359.
[25] A.A. Aldana, B. Barrios, M. Strumia, S. Correa, M. Martinelli, Dendronization of chitosan films: surface characterization and biological activity, React. Funct. Polym. 100 (2016) 18–25.
[26] M. Calderón, L.M.A. Monzón, M. Martinelli, A.V. Juarez, M.C. Strumia, L.M. Yudi, Electrochemical study of a dendritic family at the water/1,2-dichloroethane interface, Langmuir 24 (2008) 6343–6350.
[27] M. Martinelli, M. Calderón, C.I. Alvarez, M.C. Strumia, Functionalised supports with sugar dendritic ligand, React. Funct. Polym. 67 (2007) 1018–1026.
[28] G.N. Rimondino, E. Miceli, M. Molina, S. Wedepohl, S. Thierbach, E. Rühl, M. Strumia, M. Martinelli, M. Calderón, Rational design of dendritic thermoresponsive nanogels that undergo phase transition under endolysosomal conditions, J. Mater. Chem. B 5 (2017) 866–874.

[29] M. Molina, S. Wedepohl, E. Miceli, M. Calderón, Overcoming drug resistance with on-demand charged thermoresponsive dendritic nanogels, Nanomedicine 12 (2016) 117–129.
[30] A.S. De Leon, M. Molina, S. Wedepohl, A. Munoz-Bonilla, J. Rodriguez-Hernandez, M. Calderón, Immobilization of stimuli-responsive nanogels onto honeycomb porous surfaces and controlled release of proteins, Langmuir 32 (2016) 1854–1862.
[31] M. Molina, M. Giulbudagian, M. Calderón, Positively charged thermoresponsive nanogels for anticancer drug delivery, Macromol. Chem. Phys. 215 (2014) 2414–2419.
[32] M. Molina, S. Wedepohl, M. Calderón, Polymeric near-infrared absorbing dendritic nanogels for efficient in vivo photothermal cancer therapy, Nanoscale 8 (2016) 5852–5856.
[33] M. Du, D. Lu, Z. Liu, Design and synthesis of lipase nanogel with interpenetrating polymer networks for enhanced catalysis: molecular simulation and experimental validation, J. Mol. Catal. B Enzym. 88 (2013) 60–68.
[34] X. Liu, H. Guo, L. Zha, Study of pH/temperature dual stimuli-responsive nanogels with interpenetrating polymer network structure, Polym. Int. 61 (2012) 1144–1150.
[35] V. Koul, R. Mohamed, D. Kuckling, H.J. Adler, V. Choudhary, Interpenetrating polymer network (IPN) nanogels based on gelatin and poly(acrylic acid) by inverse miniemulsion technique: synthesis and characterization, Colloids Surf. B: Biointerf. 83 (2011) 204–213.
[36] Y. Chen, D. Ding, Z. Mao, Y. He, Y. Hu, W. Wu, X. Jiang, Synthesis of hydroxypropylcellulose-poly(acrylic acid) particles with semi-interpenetrating polymer network structure, Biomacromolecules 9 (2008) 2609–2614.
[37] N. Sahiner, W.T. Godbey, G.L. McPherson, V.T. John, Microgel, nanogel and hydrogel–hydrogel semi-IPN composites for biomedical applications: synthesis and characterization, Colloid Polym. Sci. 284 (2006) 1121–1129.
[38] E. Miceli, M. Kar, M. Calderón, Interactions of organic nanoparticles with proteins in physiological conditions, J. Mater. Chem. B 5 (2017) 4393–4405.
[39] K. Obst, G. Yealland, B. Balzus, E. Miceli, M. Dimde, C. Weise, M. Eravci, R. Bodmeier, R. Haag, M. Calderón, N. Charbaji, S. Hedtrich, Protein corona formation on colloidal polymeric nanoparticles and polymeric nanogels: impact on cellular uptake, toxicity, immunogenicity, and drug release properties, Biomacromolecules 18 (2017) 1762–1771.
[40] Z. Gu, A. Biswas, M. Zhao, Y. Tang, Tailoring nanocarriers for intracellular protein delivery, Chem. Soc. Rev. 40 (2011) 3638–3655.
[41] X. Liu, C.N. Kim, J. Yang, R. Jemmerson, X. Wang, Induction of apoptotic program in cell-free extracts: requirement for dATP and cytochrome c, Cell 86 (1996) 147–157.
[42] A. Matapurkar, Y. Lazebnik, Requirement of cytochrome c for apoptosis in human cells, Cell Death Differ. 13 (2006) 2062–2067.
[43] J. Mendez, M. Morales Cruz, Y. Delgado, C.M. Figueroa, E.A. Orellano, M. Morales, A. Monteagudo, K. Griebenow, Delivery of chemically glycosylated cytochrome c immobilized in mesoporous silica nanoparticles induces apoptosis in HeLa cancer cells, Mol. Pharm. 11 (2014) 102–111.
[44] B. Zhang, Z. Luo, J. Liu, X. Ding, J. Li, K. Cai, Cytochrome c end-capped mesoporous silica nanoparticles as redox-responsive drug delivery vehicles for liver tumor-targeted triplex therapy in vitro and in vivo, J. Control. Release 192 (2014) 192–201.
[45] M. Morales-Cruz, C.M. Figueroa, T. González-Robles, Y. Delgado, A. Molina, J. Méndez, M. Morales, K. Griebenow, Activation of caspase-dependent apoptosis by intracellular delivery of cytochrome c-based nanoparticles, J. Nanobiotechnol. 12 (2014) 33.
[46] S. Li, J. Zhang, C. Deng, F. Meng, L. Yu, Z. Zhong, Redox-Sensitive and intrinsically fluorescent photoclick hyaluronic acid nanogels for traceable and targeted delivery of cytochrome c to breast tumor in mice, ACS Appl. Mater Interf. 8 (2016) 21155–21162.
[47] J. Chen, Y. Zou, C. Deng, F. Meng, J. Zhang, Z. Zhong, Multifunctional click hyaluronic acid nanogels for targeted protein delivery and effective cancer treatment in vivo, Chem. Mater. 28 (2016) 8792–8799.